This chapter contains the final results of the stability tests presented in Chapter **??** along with the final diffusion length estimates, based on the results of the stability tests and general considerations and observations made throughout the thesis. Finally these σ estimates are used to give a first estimate of the temperature for the given depth interval.

Site	λ_{LT} [m]
A	0.311 ± 0.006
B	0.326 ± 0.008
D	0.354 ± 0.012
E	0.246 ± 0.005
G	0.264 ± 0.006

Table 0.1: Spectral analysis estimated annual layer thickness at the depth sections between Laki and Tambora.

0.1 Annual Layer Thickness

The final annual layer thickness estimates are determined with a section length of $l_{\mathrm{sec}} = 7$ m and a shift of $l_{\mathrm{shift}} = 1.5$ m. From Table 0.1 it can be seen that λ is smallest for Site E and Site G, which corresponds well with those sites having the lowest accumulation rates.

0.2 Diffusion Length Estimates

Before revealing the final σ estimates, the results of the stability tests carried out are presented. This concerns the effects on the diffusion length by the different spectral transforms, the constant or variable σ, and using constraints or not. The results are presented with both the optimal found diffusion length, the afterwards corrected firn diffusion length and, for some tests, the average run time for the algorithm. In Table 0.2 the average sample sizes in the Laki to Tambora depth interval used for σ_{firn} estimates can be seen.

Site	$\bar{\Delta}_z$ [cm]
A	3.92 ± 0.06
B	3.89 ± 0.06
D	3.77 ± 0.06
E	4.25 ± 0.07
G	4.10 ± 0.07

Table 0.2: Average sampling size in the depth between Laki and Tambora events.

0.2.1 Diffusion Length Estimates if Constrained or Not Constrained

The previous chapter presented the constrained method for optimization. The results of both constrained and unconstrained optimization can be seen in Table 0.3. If the method does not impose constraints on the algorithm, the algorithm is not quite as stable, as can be seen on the average run time and the run time variances. Furthermore, the unconstrained method systematically results in a diffusion length estimate lower than the one computed through the constrained method, and generally with a higher variance.

0.2.2 Diffusion Length Estimates vs. Counted Peaks

To get an understanding of how the diffusion length affected the number of counted years, a run was made going through all diffusion lengths from 1 cm to 15 cm for all cores. Illustrations of the results can be seen in Figures 0.1 and

			No Constraints	Constraints
Site A	σ_{opt}	[cm]	6.69 ± 0.85	7.88 ± 0.66
	σ_{firn}	[cm]	6.58 ± 0.87	7.79 ± 0.66
	t	[s]	19.85 ± 10.39	8.84 ± 1.47
Site B	σ_{opt}	[cm]	5.98 ± 0.24	7.31 ± 0.18
	σ_{firn}	[cm]	5.86 ± 0.24	7.21 ± 0.18
	t	[s]	11.66 ± 4.46	8.68 ± 1.08
Site D	σ_{opt}	[cm]	4.35 ± 0.53	6.94 ± 0.24
	σ_{firn}	[cm]	4.24 ± 0.32	6.84 ± 0.24
	t	[s]	14.83 ± 8.50	9.19 ± 0.72
Site E	σ_{opt}	[cm]	6.20 ± 0.20	8.15 ± 0.11
	σ_{firn}	[cm]	6.07 ± 0.21	8.05 ± 0.11
	t	[s]	5.44 ± 1.82	6.97 ± 0.56
Site G	σ_{opt}	[cm]	8.55 ± 0.27	9.35 ± 0.26
	σ_{firn}	[cm]	8.46 ± 0.28	9.27 ± 0.26
	t	[s]	29.99 ± 3.81	7.19 ± 0.48

Table 0.3: Optimal and corrected firn diffusion length estimates with either the non-constrained or the constrained method.

0.2. In Figure 0.1 it can be seen that the number of counted peaks generally increases as the diffusion length increases, until some value where the counts start being more irregular. When looking at Figure 0.2, it can be seen that for most of the cores, there exists a stable plateau of diffusion lengths that all result in $N_P = 33$, for some longer than for others. This could be used as a stability measure and a sanity check of the number of years assumed is actually likely in this section.
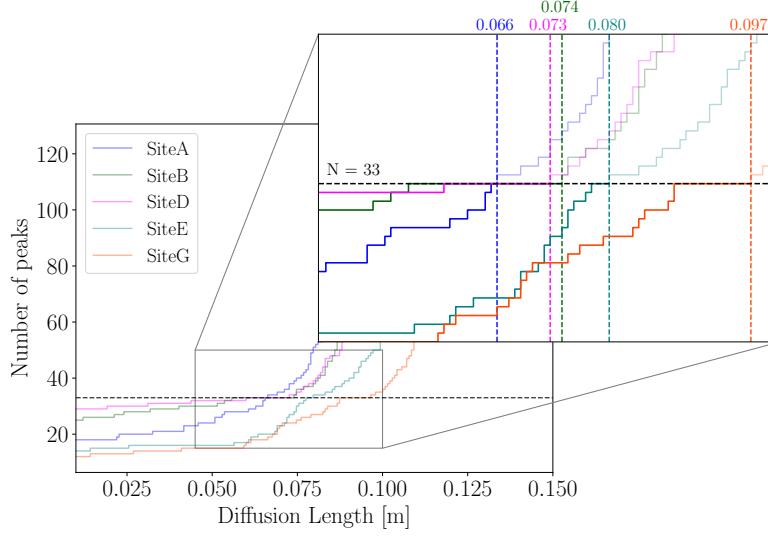
Figure 0.2: A zoom-in of the N peaks v. diffusion length plot in Figure 0.1. Specifically in focus are the maximal diffusion lengths corresponding to $N_{\text{peaks}} = 33$.

0.2.3 Diffusion Length Estimates vs. Spectral Transform Methods

In Table 0.4 the estimated diffusion lengths, both optimal and firn, are presented along with the average run time of the method. The error is estimated through drawing the Laki and Tambora event locations from a Gaussian distribution with standard deviation of two months. For all sites, the results of all three methods are almost within each other's margins. This might point to choosing one of the faster back diffusion methods to estimate the diffusion length with, if it is used for a quantitative measure. If it is needed to reconstruct a single data series one time, it might be preferable to use the NDCT.

0.2.4 Diffusion Length Estimates if Diffusion Length Constant or Variable

Deconvolution with a variable diffusion length has not been quantitatively examined, but a qualitative example of the difference between deconvolution with a constant or variable Gaussian filter can be seen in Figure 0.3. It is mostly presented here to emphasize that using either a constant or a variable σ does not result in a large difference in the restored signal. The change in
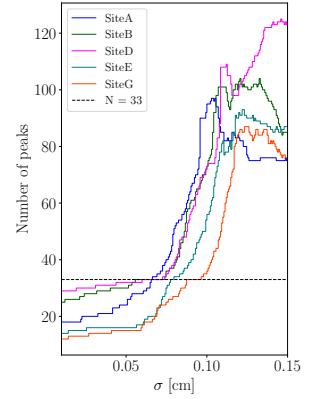

Figure 0.1: Number of peaks estimated given diffusion length, based on diffusion length in the interval [0.01; 0.15] m.

			FFT	DCT	NDCT
Site A	σ_opt	[cm]	7.57 ± 0.60	7.80 ± 0.68	7.26 ± 0.53
	σ_firn	[cm]	7.48 ± 0.61	7.71 ± 0.69	7.17 ± 0.54
	t	[s]	8.00 ± 0.91	7.93 ± 0.91	17.46 ± 0.98
Site B	σ_opt	[cm]	7.11 ± 0.40	7.30 ± 0.20	7.36 ± 0.21
	σ_firn	[cm]	7.01 ± 0.40	7.21 ± 0.20	7.27 ± 0.22
	t	[s]	8.64 ± 0.51	8.41 ± 0.82	19.06 ± 0.55
Site D	σ_opt	[cm]	7.00 ± 0.41	6.96 ± 0.28	7.21 ± 0.27
	σ_firn	[cm]	6.91 ± 0.41	6.86 ± 0.29	7.12 ± 0.27
	t	[s]	9.24 ± 0.73	9.20 ± 0.69	19.55 ± 1.03
Site E	σ_opt	[cm]	8.07 ± 0.01	8.15 ± 0.11	8.21 ± 0.14
	σ_firn	[cm]	7.97 ± 0.01	8.05 ± 0.11	8.11 ± 0.14
	t	[s]	7.28 ± 0.36	7.03 ± 0.56	16.61 ± 0.54
Site G	σ_opt	[cm]	9.38 ± 0.32	9.35 ± 0.25	9.44 ± 0.24
	σ_firn	[cm]	9.29 ± 0.32	9.27 ± 0.25	9.36 ± 0.24
	t	[s]	7.53 ± 0.49	7.24 ± 0.49	16.45 ± 0.34

Table 0.4: Diffusion length estimates resulting in $N_\text{peaks} = 33$ based on different spectral transform methods, namely the FFT, DCT and NDCT presented in earlier chapters and described in Appendix **??**. Along with the optimal diffusion length, the actual firn diffusion length is presented - corrected for sampling diffusion, ice diffusion and thinning. The computational time of the back diffusion process given the different spectral transforms is also presented.

theoretically estimated $\sigma(z)$ at the depths under consideration here is relatively small, resulting in a small difference from the constant σ. It is thus concluded that the speed is prioritized in the σ estimations and the variable $\sigma(z)$ method is abandoned.
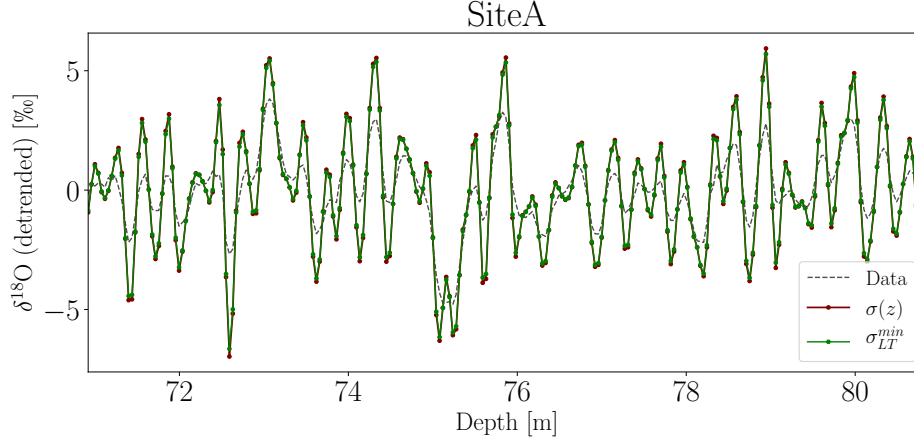
Figure 0.3: Backdiffused data, deconvolution with $\sigma_{\text{constant}} = \sigma_{\text{LT}}^{\min}$ and $\sigma(z)$.
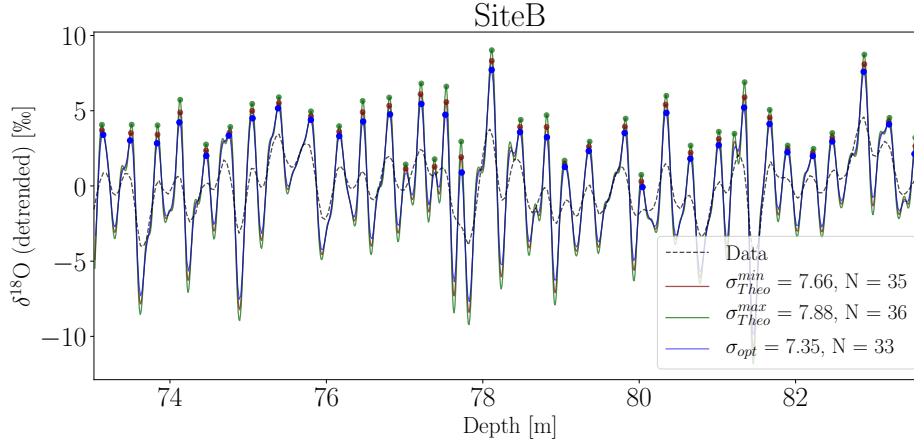

Figure 0.4: Example of back diffused data from Site A, both deconvoluted with maximum and minimum expected σ and with the final σ_{opt}.

0.2.5 Final σ Estimates Based on Previous Conclusions

Figure 0.4 shows the optimal diffusion length estimate resulting in $N_P = 33$ for Site B, along with the restorations using the theoretical diffusion length estimates, $\sigma_{\min}$ and $\sigma_{\max}$, in the Gaussian filter. The theoretical estimates are not resulting in an unlikely number of peaks, but the optimization algorithm still estimates a lower diffusion length, resulting in the wanted 33 peaks.

			σ_{final}	σ_{Fit}	σ_{Theo}
Site A	σ_{opt}	[cm]	7.37 ± 0.54	7.12	$-$
	σ_{firn}	[cm]	7.27 ± 0.55	$-$	$[7.69; 7.90]$
Site B	σ_{opt}	[cm]	7.35 ± 0.22	7.42	$-$
	σ_{firn}	[cm]	7.26 ± 0.22	$-$	$[7.58; 7.80]$
Site D	σ_{opt}	[cm]	7.21 ± 0.28	7.56	$-$
	σ_{firn}	[cm]	7.12 ± 0.28	$-$	$[7.36; 7.54]$
Site E	σ_{opt}	[cm]	8.22 ± 0.15	7.81	$-$
	σ_{firn}	[cm]	8.12 ± 0.15	$-$	$[8.85; 9.13]$
Site G	σ_{opt}	[cm]	9.46 ± 0.24	8.21	$-$
	σ_{firn}	[cm]	9.38 ± 0.24	$-$	$[8.85; 9.10]$

Table 0.5: Final diffusion length estimates, based on conclusions made previously in different tests, along with theoretical and fit estimates.

In Table 0.5 the final optimized diffusion length estimates can be seen, along with the theoretical diffusion length interval and the σ estimated from the fit to the PSD of the signal.

0.3 Final Temperature Estimates from Optimal Estimated σ

The temperature estimates are, as described previously, made based on a steady state model, with a constant accumulation rate. The estimate is then made numerically through a Newton-Raphson scheme from `scipy.optimize.newton`, finding the roots of $\sigma_{\text{model}} \cdot \frac{\rho_{\text{CO}}}{\rho_{\text{ice}}} - \sigma_{\text{data}}$.

The final temperature estimates can be seen in Table 0.6 and the underlying distributions in Figure 0.5. Again in these distributions can the quantization of the results can be seen, resulting in non-Gaussian distributions.

The final temperatures have been presented along with the assumed temperature, T_0, which has been used to generate modelled density and diffusion length profiles previously in this work and is the steady state assumed surface temperature at the sites.

		Site A	Site B	Site D	Site E	Site G
T_0	[$^{\mathrm{o}}$C]	-29.41	-29.77	-28.3	-30.37	-30.1
$\bar{T}_{\mathrm{StSt}}^{\mathrm{Opt}}$	[$^{\mathrm{o}}$C]	-31.04 ± 2.02	-30.46 ± 0.83	-30.00 ± 1.05	-30.80 ± 0.48	-25.93 ± 0.70
$\bar{T}_{\mathrm{StSt}}^{\mathrm{Firn}}$	[$^{\mathrm{o}}$C]	-31.41 ± 2.07	-30.81 ± 0.85	-30.35 ± 1.07	-31.14 ± 0.49	-26.18 ± 0.71

Table 0.6: Steady state temperature estimates based on the final firn diffusion length estimates found. T_0 is the temperature used to generate the theoretical diffusion length and density profiles, and originates from [**?**, add. text]
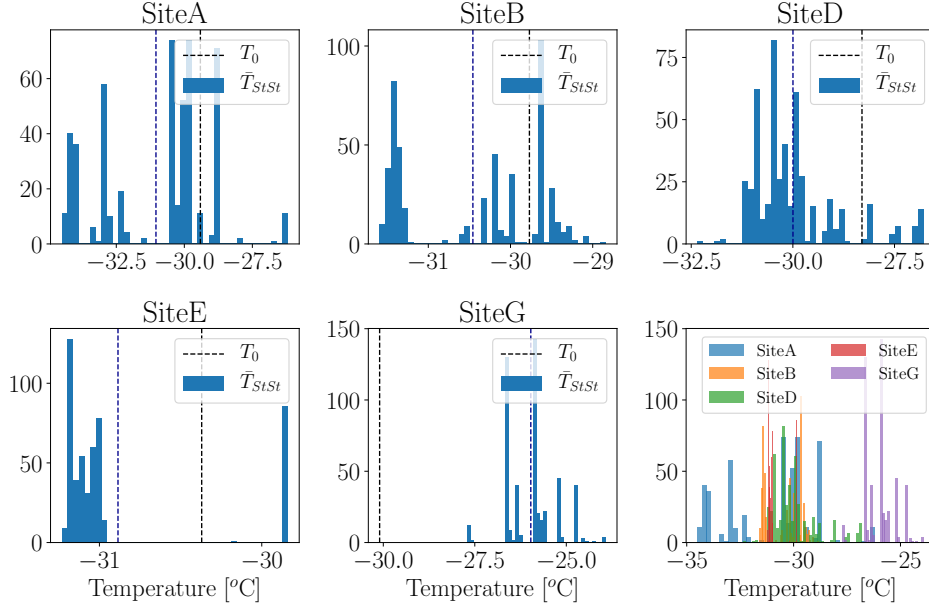

Figure 0.5: Steady state temperature distributions

0.3.1   Further Possibilities with the Iso-CFM

These temperature estimates are made on a steady state assumption, that is, that the annual accumulation rate, A_0, and surface temperature, T_0, are at a steady state. This of course is not an optimal assumption, but it is a useful stepping stone to sanity check the results and from where to continue further temperature analysis and estimations with less rigid models.

An obvious easy next step would be to investigate different accumu-

lation rates, instead of just computing for a single A_0. This will need an adjusting of the λ used in the general method and might give insight into a more accurate A_0 estimate, still under steady state assumptions.

In further analysis and work, it would be interesting to utilize the Iso-CFM to model non-steady state solutions and use these to estimate temperatures from more realistic models. This could be models implementing seasonal changes in both temperature and accumulation rate, or statistical analysis of random variations.